



City Research Online

City, University of London Institutional Repository

Citation: Stefanidou, S.P., Paraskevopoulos, E. A., Papanikolaou, V. K. & Kappos, A. J. (2022). An online platform for bridge-specific fragility analysis of as-built and retrofitted bridges. *Bulletin of Earthquake Engineering*, 20(3), pp. 1717-1737. doi: 10.1007/s10518-021-01299-3

This is the accepted version of the paper.

This version of the publication may differ from the final published version.

Permanent repository link: <https://openaccess.city.ac.uk/id/eprint/27554/>

Link to published version: <https://doi.org/10.1007/s10518-021-01299-3>

Copyright: City Research Online aims to make research outputs of City, University of London available to a wider audience. Copyright and Moral Rights remain with the author(s) and/or copyright holders. URLs from City Research Online may be freely distributed and linked to.

Reuse: Copies of full items can be used for personal research or study, educational, or not-for-profit purposes without prior permission or charge. Provided that the authors, title and full bibliographic details are credited, a hyperlink and/or URL is given for the original metadata page and the content is not changed in any way.

City Research Online:

<http://openaccess.city.ac.uk/>

publications@city.ac.uk

An online platform for bridge-specific fragility analysis of as-built and retrofitted bridges

Sotiria P. Stefanidou¹, Elias A. Paraskevopoulos¹,
Vassilis K. Papanikolaou², Andreas J. Kappos³

¹Postdoctoral Researcher, School of Civil Engineering, Aristotle university of Thessaloniki, Greece.

²Assistant Professor, School of Civil Engineering, Aristotle University of Thessaloniki, Greece.

³ Professor, Dept. of Civil Infrastructure and Environmental Engineering, Khalifa University, Abu Dhabi, UAE
(formerly, Professor, School of Civil Engineering, Aristotle University of Thessaloniki, Greece).

Abstract

Bridges are the most critical and usually the most vulnerable structural component of a road network exposed to various hazards. Damage due to recent earthquakes worldwide highlighted the substantial direct and indirect financial losses related to partial or total collapse of critical bridge components and pointed to the need for reliable assessment of their seismic performance. This paper presents a ‘toolkit’ developed for bridge-specific fragility analysis of bridges; it is implemented on a “two-track” online platform, including ad-hoc developed software for online bridge-specific fragility curve derivation, as well as the option to select an appropriate set of generic fragility curves from a database including a broad range of bridge classes. Three alternative options for the estimation of component-specific limit state thresholds are provided; selection from extensive lists with available thresholds for piers, bearings and abutments, and calculation of limit state thresholds for as-built and retrofitted piers based on (a) closed-form relationships, or (b) inelastic pushover analysis and capacity assessment of a parametrically defined pier model (carried out online). Details regarding the software developed, the methodology for bridge-specific fragility curves, and all critical features are presented and discussed herein. The application of the online software is illustrated through two case studies involving the derivation of fragility curves for bridges with different structural systems and properties.

1. INTRODUCTION

Bridges are the most critical and usually the most vulnerable structural component of a road network, exposed to natural and man-made hazards. Damage due to recent earthquakes worldwide highlighted the substantial direct and indirect financial losses related to partial or total collapse of critical bridge components and pointed to the need for a reliable assessment of their seismic performance. Over the last decades, the urban and interurban road network in Europe has been expanded; it currently includes both newly constructed and older road and railway bridges. In view of this, the need for an effective open-access tool for the assessment of bridge vulnerability has emerged. Such a tool should be

applicable to bridge portfolios, including bridges with different structural systems, geometries, and material properties, thus ensuring a broad application range; moreover, it should be able to account for structure-specific parameters in an effective and pragmatic way.

Several methodologies have been developed during the last two decades for the assessment of the seismic vulnerability of bridges, most of them in the context of developing fragility curves. The estimation of the probability of damage (or limit state exceedance) for different levels of earthquake intensity may be considered an indicator for retrofit necessity and prioritization; therefore, fragility curves of as-built and retrofitted bridges are valuable tools for decision-making. The available methodologies may be categorized as *empirical*, based on expert judgment and recorded earthquake damage, *analytical*, based on numerical analysis results, and *hybrid*, combining analysis results and empirical data. Since available bridge damage data due to earthquakes is limited for as-built and, even more so, for retrofitted bridges, most of the methodologies for the derivation of fragility curves in the literature are analytical (Billah & Alam, 2014). Analytical methods may be classified to those focusing on the derivation of generic fragility curves, applicable to typological bridge classes (e.g., DesRoches et al., 2012, Tsionis & Fardis, 2012), and those focusing on bridge-specific fragility curves (Stefanidou & Kappos, 2017). It should be noted that, in most cases, the limit state (LS) threshold values of the engineering demand parameters (typically deformation quantities) are defined based on qualitative criteria and experimental data (Hazus, 2015, Berry & Eberhard, 2003) rather than being derived from numerical analysis of the capacity of critical components (Stefanidou & Kappos, 2019). Likewise, the uncertainty values considered in fragility analysis (uncertainty in capacity and LS definition) are usually selected based on literature recommendations (Hazus, 2015), while uncertainty in seismic demand is usually quantified based on parametric analyses. Recently, analytical methodologies have been extended to retrofitted bridges, with a view to assessing the seismic behaviour of bridge systems retrofitted with various retrofit techniques and strategies, and evaluate their effectiveness. Fragility curves were derived for bridges retrofitted with reinforced concrete (RC) or FRP jackets (Bisadi et al., 2011, Mohammadi & Lahijanian, 2010), as well as for bridges with seismic isolation (high-damping bearings with lead core, friction bearings) (Zhang & Huo, 2009); moreover, fragility-informed selection of optimum retrofit schemes for specific performance criteria has been recently proposed, involving use of fragility curves for as-built and retrofitted bridges (Stefanidou & Kappos, 2021).

In view of the previous considerations, the relevance of developing a database including the fragility curves available in the literature, classified in an effective way, is clear. Attempts to develop platforms and databases of bridge fragility curves are so far limited; they include online databases and “manager tools” for fragility functions. The online database created within the GEM project (see Yepes-Estrada et al. 2016) is arguably the most systematic attempt to collect and organise fragility curves of (as-built) bridges; the database also includes RC and masonry buildings. In the frame of the research project SYNER-G, Silva et al. (2014) developed a fragility function manager tool, an interface that includes bridge fragility function lists, allowing the user to add fragility functions not included in the database. However, the database cannot be used online; the tool is available for download and should

be locally installed. It should also be noted that a comprehensive literature review on fragility curves has been carried out in the frame of other research projects (e.g., Crowley et al., 2011, D'Ayala et al., 2015), which include data regarding LS definition and threshold values for bridges and bridge components.

This paper presents an online 'toolkit' (that goes beyond a 'manager tool') developed for fragility analysis of as-built and retrofitted bridges (www.thebridgedatabase.com). For the first time, a 'two-track' platform is provided online, including ad-hoc software for online bridge-specific fragility curve derivation using a database of bridge components, as well as the option to select an appropriate set of generic fragility curves (functions) from an extended catalogue, based on the bridge class selected. The software is based on a recently proposed, component-based, structure-specific methodology (Stefanidou & Kappos, 2017) tailored to bridge portfolio fragility analysis, and was developed in Python (Van Rossum, G., & Drake, 2009) using OpenSeesPy (Zhu et al., 2018) for multiple bridge analyses. A fully parameterised bridge model was developed, allowing for input of user-defined geometry, other component parameters, and seismic excitation; it includes a probabilistic framework that considers all pertinent uncertainty sources. Within the component-based methodology, fragility curves for bridge piers, bearings, and abutments, are calculated and combined to derive system fragility (considering component series connection and providing upper and lower bound limits for system fragility, i.e., considering uncorrelated and completely correlated components). Moreover, a database and a software module for estimating LS thresholds for as-built and retrofitted bridge piers are available on the online platform. Specifically, based on experimental studies and other information available in the literature, the LS thresholds for different as-built and retrofitted bridge pier types (namely circular, hollow circular, rectangular, hollow rectangular and wall type), bearings, and abutments are embedded in the platform. The toolkit also includes the closed-form relationships described in Stefanidou & Kappos (2019), allowing a component-specific (online) estimation of LS thresholds; moreover, it provides an ad-hoc software for their analytical estimation based on pushover analysis of the fully parameterised inelastic model, considering multiple failure modes. It is pointed out that the online platform is fully interactive, allowing input from users/contributors, with a view to not only receiving feedback but also enriching the platform.

2. WEB-BASED INTERFACE AND OUTLINE OF THE BRIDGE ONLINE PLATFORM

The basic structure of the platform is shown in Fig.1, including the main menu and all submenus. The platform includes data and software for generic and bridge-specific fragility curves, while examples of software application to common types of bridges are also available. The platform will be extended to include machine learning techniques at a later stage of development.

A detailed catalogue is provided of *generic* fragility curves, classified based on critical parameters such as bridge typology, engineering demand parameters, intensity measures, etc. The bridge typologies included are classified according to the classification scheme proposed by Moschonas et al., 2008 and

are summarised within a selective list; the user may directly select the bridge typology from the list. The fragility curve catalogue is interactive, allowing the users to submit online data for new fragility curves that will be included in the database after proper review. For *bridge-specific* fragility analysis, the platform provides alternatives for the calculation of critical component (pier) capacity, detailed estimation of uncertainty in seismic capacity and LS definition for all critical components, and online software for the calculation of bridge-specific fragility curves based on user-defined input parameters for the bridge and the seismic action. Regarding the estimation of critical component capacity, three alternatives are available for as-built and retrofitted piers and one for bearings and abutments. For any pier section type, the user may estimate the LS threshold values online, applying the closed-form relationships proposed in Stefanidou & Kappos (2019), select the values from the database developed based on an extensive review of literature on LS, or estimate the LS thresholds based on inelastic pushover analysis of each pier. For the case of bearings and abutments, the LS thresholds may be selected from a detailed database available online, including definitions proposed in the literature. In the platform for *bridge-specific* fragility analysis, default values for LS thresholds for piers, bearings, and abutments are included (closed-form relationships for piers, and values for bearings and abutments proposed in Stefanidou & Kappos 2017, 2019), while the option for user-defined input values is also available.

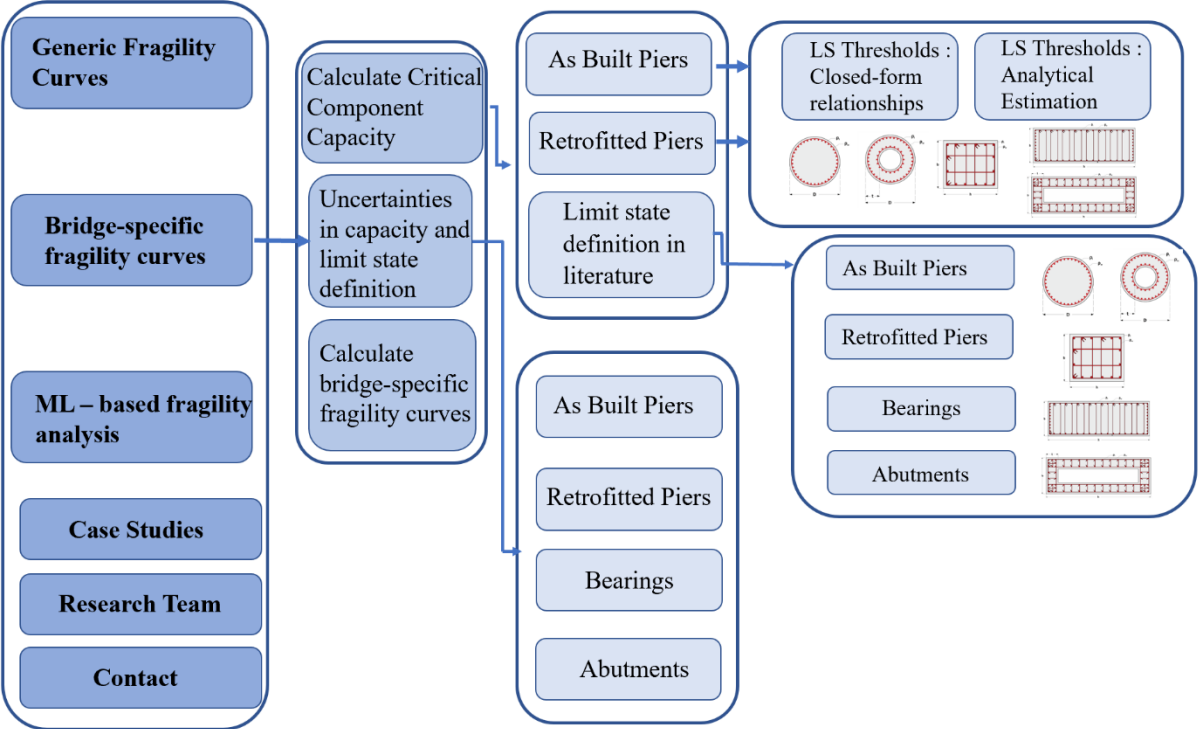


Figure 1. Modules of the online platform including the generic fragility curve database and the software and data for bridge-specific fragility analysis.

3. GENERIC FRAGILITY CURVE DATABASE

The first module of the online platform is for the estimation of fragility curves for a bridge by classifying it to a specific typological class and selecting appropriate curves for this class. The bridges included in the database are classified according to a scheme that is an extended version of that suggested by Moschonas et al., 2008. A catalogue of existing generic fragility curves for various typological classes is included in the database; they were derived numerically in studies carried out in the last two decades. The database includes links to each pertinent publication, as well as a standard form for each; the bridge typologies addressed in each publication are the first parameter in the form, which also includes material and structural characteristics of the bridge. Additional parameters that affect the fragility curve development are also included, namely the critical components considered for bridge fragility estimation, the engineering demand parameters, and the threshold values selected for each component or at system level, as well as modelling and analysis method information. Details regarding the seismic input motion are also included, along with issues related to the ‘format’ of the fragility curve, i.e., the parameter of seismic intensity in terms of which the fragility function is derived and the adopted uncertainty values.

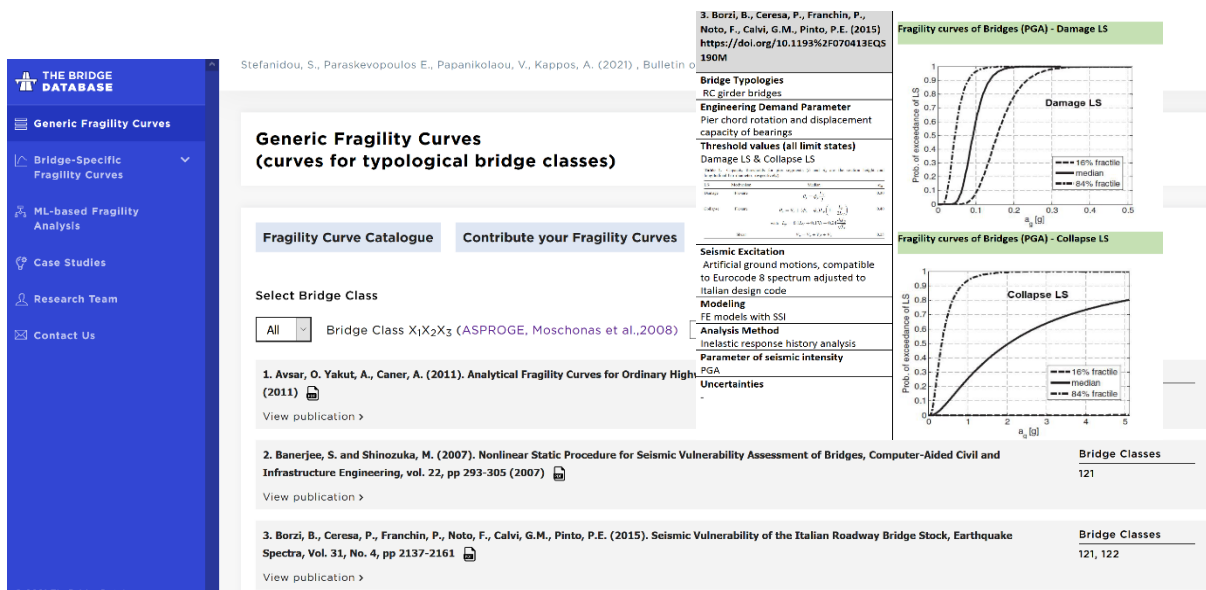


Figure 2. Online catalogue of generic fragility curves for typological bridge classes

The generic curve webpage and a typical standard form are shown in Fig.2. The user selects a typological class from the drop-down menu at the top, and the existing curves for this typology are displayed (references, links to publications, and standard forms). A quick look at the form for each set of curves assists the user in selecting (if there are more than one sets for the class) the one that is more appropriate for their needs.

4. BRIDGE -SPECIFIC FRAGILITY CURVES

The second (and most important) module of the platform is the one for online, real-time, structure-specific calculation of bridge fragility curves. In the frame of the component-based methodology for the estimation of fragility curves (Stefanidou & Kappos, 2017), capacity and demand for all critical components should be considered, and all sources of uncertainty should be quantified. Several features are provided within the platform, including the calculation of component-specific capacity and LS thresholds (either analytical, based on closed-form relationships, or adopted from the literature) and the estimation of uncertainties in capacity and LS definition. For a large number of bridge classes, the uncertainty in seismic demand was estimated for every component based on inelastic response history analysis by Stefanidou & Kappos, 2019, and these values are included in the database (in addition to those from the literature, see Section 3). The user can either calculate bridge-specific fragility curves online or just extract from the database LS thresholds (quantifying damage for different limit states) and uncertainties, to be used in alternative methodologies for fragility curve development.

4.1. Capacity and LS thresholds for as-built and retrofitted piers

The calculation of seismic capacity and LS thresholds is available on the platform for both as-built and retrofitted bridge piers of various types. Three alternatives are included, namely the estimation of LS thresholds based on closed-form relationships proposed in Stefanidou & Kappos (2019), their estimation based on literature recommendations, and their online calculation based on capacity assessment through inelastic pushover analysis of the inelastic pier model.

4.1.1. Closed-form relationships for the estimation of LS thresholds

The estimation of LS threshold values in displacement terms for RC as-built and retrofitted piers is possible using the closed-form relationships provided on the platform. Different relationships are included for the quantitative definition of minor to major damage thresholds of various pier types, namely cylindrical, hollow cylindrical, rectangular, hollow rectangular, and wall-type piers (Fig. 3). The closed-form relationships are based on regression analysis of extensive parametric inelastic (pushover) analysis results, considering different failure modes (flexural and shear). Critical parameters affecting the seismic capacity of bridge piers were considered as variables (pier type, dimension, material properties, reinforcement ratio, etc.); a range of values for each parameter was selected, and multiple models were set up and analysed. Details regarding the distinct steps for the derivation of the closed-form relationships can be found in Stefanidou & Kappos (2019) and Stefanidou & Kappos (2021) for as-built and retrofitted piers, respectively, along with details of modelling issues and the qualitative and quantitative definition of damage in local (section curvature) and global (pier displacement) terms.

Damage thresholds are initially defined in terms of local engineering demand parameters (curvature, strain) and are subsequently mapped onto global ones (displacement of control point) via inelastic

analysis of the bridge pier model, considering that inelastic deformation is concentrated at the plastic hinge (bilinear $M-\phi$ curve). To estimate the bilinear $M-\phi$ curve, used as input at the plastic hinge location, section analyses are performed for all pier sections considered, accounting for varying geometry, material, reinforcement, and loading parameters (all possible combinations). So long as the results in terms of moment-curvature are available, regression is performed, and closed-form relationships for yield and ultimate moment and curvature are derived; these relationships are included in the database. The LS thresholds for as-built and retrofitted bridge piers in displacement terms ($d_1 \sim d_4$), estimated according to the closed-form relationships described previously, are included as default values in the software for the online estimation of bridge-specific fragility curves.

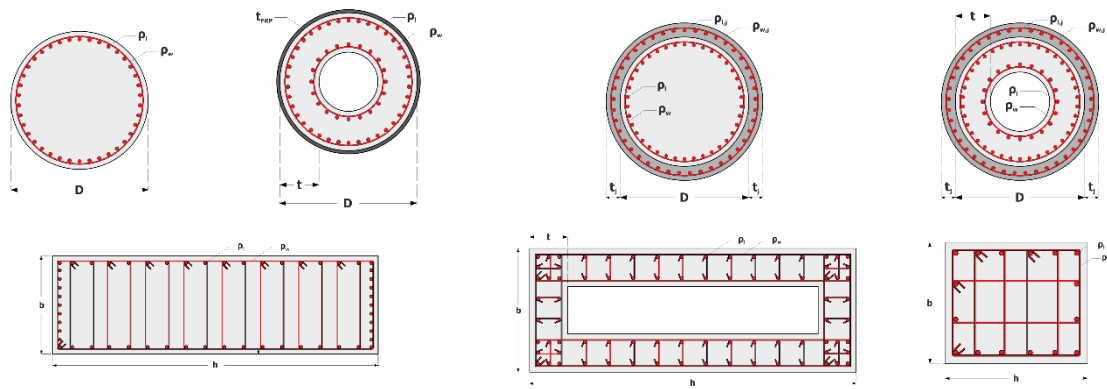


Figure 3. Different as-built pier types considered in the database for which closed-form relationships are provided for their LS thresholds

The closed-form relationships included in the database are illustrated in Fig. 4 for the case of cylindrical piers. Similar relationships are available for all limit states (LS1 to LS4, i.e. minor damage to collapse) and all different pier section types (cylindrical, hollow cylindrical, rectangular, hollow rectangular, and wall-type). All input parameters are explained in the database, and the parameter range considered is also provided. Moreover, closed-form relationships are provided for retrofitted piers, namely cylindrical and hollow cylindrical piers retrofitted with RC and FRP jackets. Details regarding the assumptions and parameters of retrofitted pier sections (confined concrete, retrofit parameters, etc.) are provided in Stefanidou & Kappos (2021).

It should be noted that the proposed relationships are based on regression analysis of results for cantilever pier models. However, depending on the structural system and the deck stiffness (in monolithic joints) or bearing stiffness (in non-monolithic deck to pier connections), the moment at the pier top may be non-zero. In this case the threshold values estimated from the closed-form relationships in the platform should be modified according to Eq.1 (from Stefanidou & Kappos 2017), a feature included in the online software)

$$d_{(L)} = \left(\frac{6x-2}{4 \cdot x^3} \right) \cdot d_{(L_0)} \quad (1)$$

Closed-form relationships d/h

$$\frac{d}{H} = \exp \left[\beta_0 + \beta_1 \cdot \ln \left(\frac{D}{H} \right) + \beta_2 \cdot \ln(v) + \beta_3 \cdot \ln \left(\frac{f_c}{f_y} \right) + \beta_4 \cdot \ln \rho_w + \beta_5 \cdot \ln \rho_l \right]$$

► **d₁/H Calculation**

	β_0	β_1	β_2	β_3	β_4	β_5
d ₁ /H	-6.524	-0.876	-0.018	-0.688	0.086	0.292

Please fill in the following parameters and press "Calculate".

ρ_l : _____ ρ_w : _____ D (m): _____ f_c (MPa): _____ f_y (MPa): _____ v: _____ H (m): _____

Calculate

d₁/H : _____

Figure 4. Online form for the estimation of LS thresholds for cylindrical piers in terms of displacement ($d_1 \sim d_4$)

4.1.2. Analytical estimation of LS thresholds

An alternative for the online estimation of LS threshold values in displacement terms for RC as-built and retrofitted piers is available in the database; it is based on inelastic static (pushover) analysis carried out on the platform. A detailed fully parameterised inelastic model has been developed in OpenSees.py (Zhu et al., 2018) supplemented by an ad-hoc software in Python (Van Rossum, G., & Drake, 2009) to estimate all key parameters (i.e., confined concrete properties, section aggregator properties, etc.) and process the analysis results. Inelastic pushover analysis using the OpenSees.py model is performed, and the pushover curve is provided, along with LS threshold values in displacement terms, i.e., displacement of the control point (d_1 to d_4), quantitatively defining minor damage to collapse for the as-built or retrofitted (with RC or FRP jacket) pier.

Numerical estimation of LS thresholds is available for as-built cylindrical and rectangular piers and for cylindrical piers retrofitted with RC and FRP jackets. All critical parameters related to member and cross-section geometry, and the axial loading are considered as variables (Fig.5e); they are entered in online forms and used as input to the parametrically defined inelastic model developed in OpenSees.py. A fully inelastic model of the cantilever pier is set up, considering distributed plasticity (fiber model) at the pier base. The number of fibers along the section perimeter is defined (defaults are included), and all material and reinforcement properties are provided. For the concrete material model, unconfined properties are provided and used as input for the concrete cover, while confined concrete properties are used as input for the concrete core; they are estimated according to (a) the Mander et al. (1988) model for cylindrical pier sections, (b) the confined concrete model of EC2 (CEN, 2004) for rectangular piers, and (c) the Spoelstra & Monti (1999) model for FRP-retrofitted cylindrical pier sections. It should be

noted that for the RC jacketed pier sections, a 50% reduction in core confinement was applied to avoid the ‘double’ core confinement effect (core and jacket transverse reinforcement), described in Stefanidou & Kappos (2021). Shear capacity is also considered by defining the $V-\gamma$ (shear force vs. shear deformation) curve according to Mergos & Kappos (2009), which is used as input at plastic hinge location, entered via section aggregator. The parameters of the $V-\gamma$ curve are calculated according to Kowalsky & Priestley (2001) and EC2 (CEN, 2004) for cylindrical and rectangular pier sections, respectively, and according to the Greek Code for Structural Interventions KANEPE (2017) for RC and FRP retrofitted sections. Based on the input parameters described above, a case-specific inelastic pier model is set up, and inelastic pushover analysis is performed for the target displacement provided by the user (again, defaults are included). The LS thresholds are initially estimated in terms of a local parameter (material strain and corresponding curvature values), as defined in Stefanidou & Kappos (2017). During analysis, the displacement at the step where the local parameter threshold is exceeded is recorded; therefore all LS thresholds are estimated in displacement terms and are marked on the pushover curve ($d_1 \sim d_4$ values). This software module of the platform may be used for pushover analysis of a pier and LS threshold estimation, irrespective of the methodology applied for fragility analysis. It should be noted that these values refer to the equivalent cantilever, therefore Eq.1 should be applied for the estimation of LS thresholds of end-restrained piers.

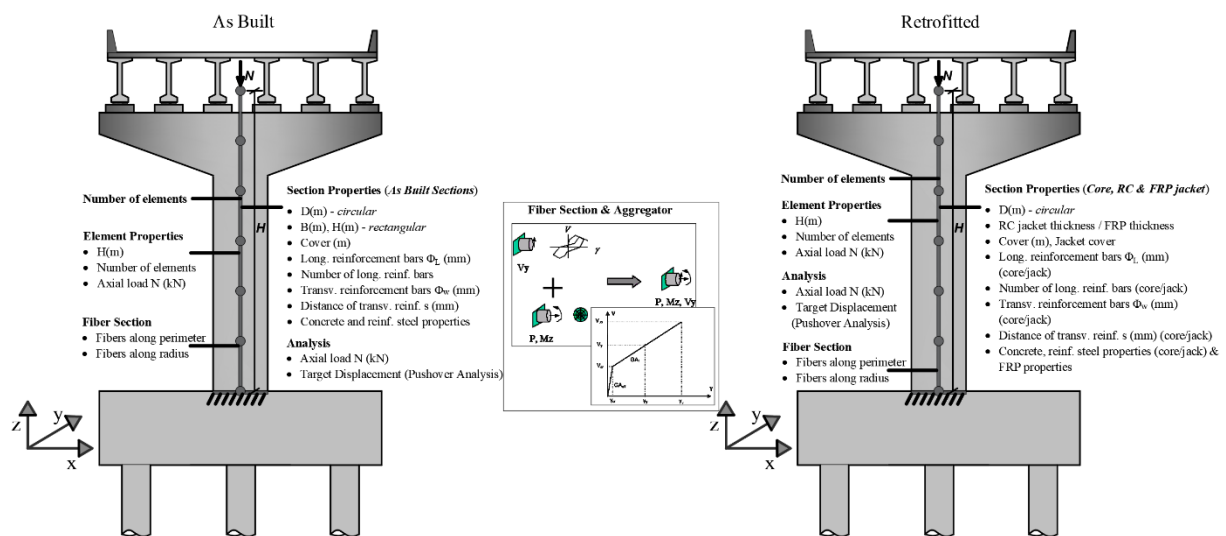


Figure 5. Input parameters for as-built and retrofitted piers and analytical estimation of LS thresholds (see <https://thebridgedatabase.com/bridge-specific/capacity/as-built-piers/ls-analytical/> for full-size figures)

4.1.3. LS threshold definitions from the literature

In addition to the numerical estimation and closed-form equations, the platform provides extensive lists with literature recommendations for the definition of LS thresholds. The pertinent references are classified according to the engineering demand parameter used (drift or displacement ductility). At the same time, qualitative and quantitative definition of LS thresholds is provided, along with loading type

and specimen characteristics. The qualitative definitions of damage in the literature are matched to the limit state thresholds (LS1~ LS4) described in Stefanidou & Kappos (2017) for all references listed in the database.

The LS thresholds based on literature recommendations (Fig. 6) are provided in tables for all different pier types, i.e., cylindrical, hollow cylindrical, rectangular, and hollow rectangular piers, as well as for cylindrical piers retrofitted with RC and FRP jackets.

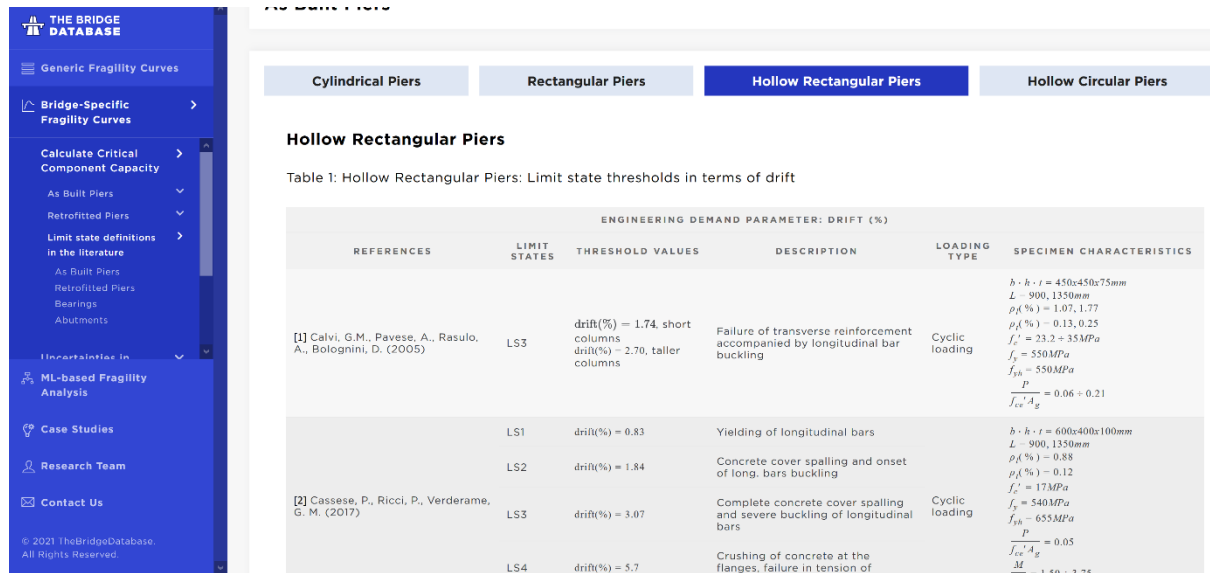


Figure 6. LS threshold values for bridge piers based on literature recommendations.

4.2. Capacity and LS thresholds for bearings and abutments

As the methodology for bridge-specific fragility analysis is component-based, the seismic capacity of all critical (for the seismic behaviour) components should be estimated in order to calculate both component and system fragility. To this end, LS thresholds for bearings and abutments are provided in the database for different bridge bearing types, namely elastomeric, elastomeric with PTFE, lead rubber, and steel bearings, in terms of shear deformation, as well as for seat-type abutments in terms of displacement, expressed as a percentage of the backwall height. The quantitative definition of damage (LS thresholds) along with the qualitative damage description and mapping onto the limit states (LS1~ LS4), defined in Stefanidou & Kappos (2017), are also available online. These values were derived by processing information available in previous studies, mainly experimental; all pertinent references are listed in the database.

4.3. Uncertainties in seismic capacity and LS definition for critical components

The estimation of uncertainty is a crucial (and often inadequately addressed) issue in fragility analysis and requires quantifying several sources, such as capacity, demand, and limit state definition. In the frame of bridge-specific fragility analysis, the seismic fragility of all critical components should be estimated; therefore, the total uncertainty associated with each component may be defined (assuming that the uncertainties are uncorrelated) as

$$\beta_{tot,comp} = \sqrt{\beta_{C,comp}^2 + \beta_{D,comp}^2 + \beta_{LS,comp}^2} \quad (2)$$

Uncertainties in seismic capacity are calculated based on the processing of analysis results for critical components (e.g. pushover analysis of bridge piers), while uncertainty in limit state definition is quantified based on statistical processing of limit state threshold values proposed in the literature. Uncertainty in seismic demand is quantified for all critical components based on inelastic response-history analysis results and is presented in Stefanidou & Kappos (2019) for representative bridges of several typological classes (according to the classification scheme mentioned in Section 3).

4.3.1. Uncertainties in capacity and LS definition for as-built and retrofitted bridge piers

The uncertainty in seismic capacity (β_c) of as-built and retrofitted bridge piers has been quantified in Stefanidou & Kappos (2017), based on the processing of inelastic pushover analyses results of a representative sample for each type, generated using Latin Hypercube sampling. The β_c values are calculated for all different pier types, and the results are available in the platform for each limit state ($\beta_{c,LS1} \sim \beta_{c,LS4}$). The mean value $\beta_{c,mean}$ for all limit states, is also provided, ranging from 0.31 to 0.41 for each pier type. Therefore, consideration of a uniform value equal to 0.35 irrespective of pier type and LS is a pragmatic option.

Statistical analysis of the data regarding the various definitions of LS in the literature provided estimates of the mean, standard deviation, and hence the β_{LS} values for bridge piers of all common types. The β_{LS} values were quantified for all limit states and different pier types considering the most frequently used engineering demand parameter, namely the pier drift. The results are presented in Table 1 and Fig. 7 for all pier types; the average β_{LS} values range from 0.20 to 0.41, depending on the pier type. It should be noted that the uncertainty in LS definition for bridge piers has also been quantified in Stefanidou & Kappos (2017), considering different engineering demand parameters (EDPs) available in the literature for bridge piers irrespectively of pier type. The β_{LS} values for different EDPs, namely drift, displacement ductility, rotational ductility, and curvature ductility, are provided in the database; they range from 0.20 to 0.43. Therefore consideration of a uniform β_{LS} value equal to 0.30 irrespective of pier type, EDP, and LS, is deemed as a pragmatic option. Values of average β_c and β_{LS} were also calculated for retrofitted

bridge piers, and the recommended constant values are the same as the ones derived for the as-built piers.

Table 1. Uncertainties in LS definition for different pier types considering drift (%) as EDP – Statistical analysis of LS definitions in the literature, available in the database.

	Cylindrical Piers - d/h (%)				Rectangular Piers - d/h (%)				Hollow Cylindr. Piers - d/h (%)				Hollow Rect. Piers - d/h (%)			
	LS1	LS2	LS3	LS4	LS1	LS2	LS3	LS4	LS1	LS2	LS3	LS4	LS1	LS2	LS3	LS4
Mean	0.83	1.98	4.26	6.25	0.83	2.26	3.96	4	1	2.75	4.85	–	0.7	2.7	3.35	–
Stand. Dev.	0.16	0.88	0.52	1.77	0.31	1.25	1.3	1.41	0	0.66	1.77	–	0.24	1.46	1.36	–
COV	0.2	0.45	0.12	0.28	0.38	0.55	0.33	0.35	0	0.24	0.36	–	0.34	0.54	0.4	–
β_{LS}	0.19	0.43	0.12	0.28	0.36	0.52	0.32	0.34	0	0.24	0.35	–	0.33	0.51	0.39	–
Average β_{LS} (LS1-LS4)	0.25				0.39				0.2				0.41			

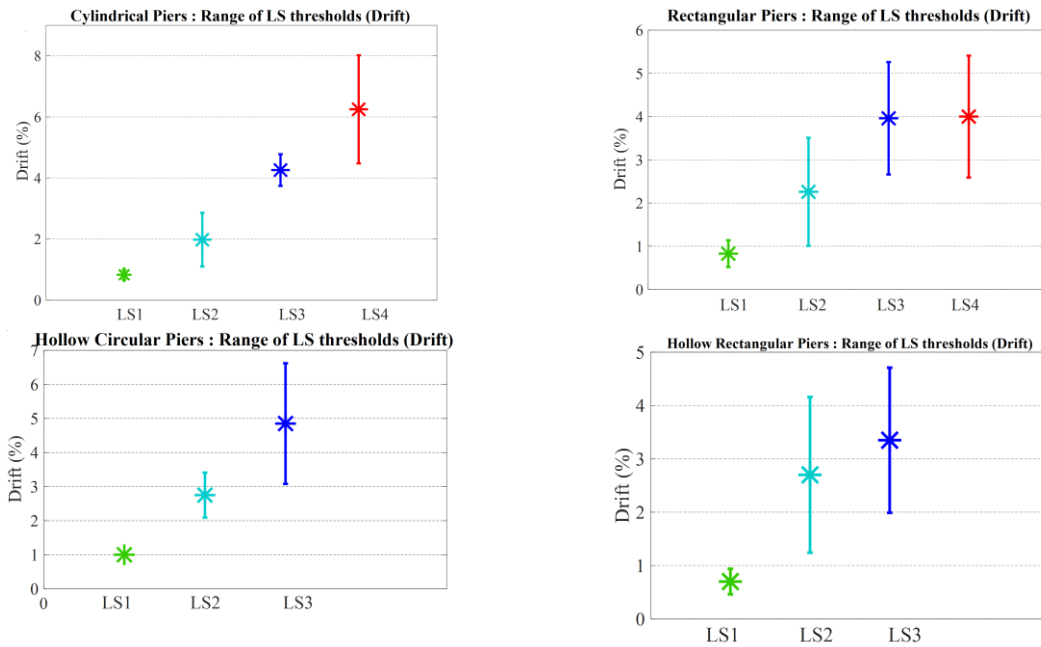


Figure 7. Range of LS thresholds for cylindrical, hollow cylindrical, rectangular, and hollow rectangular piers.

4.3.2. Uncertainties in capacity and LS definition for bearings and abutments

The online platform provides extensive data from the literature for the limit state threshold values for different bearing types in terms of shear deformation, and for seat-type abutments in terms of top displacement (expressed as a percentage of the backwall height). Statistical analysis of the data collected was performed and led to the estimation of β_{LS} values for all limit states. The results are presented in Table 2 and Fig. 8, and it is seen that consideration of a constant β_{LS} equal to 0.35 and 0.40 for elastomeric bearings and abutments, respectively, is a pragmatic option. It should be noted that the β_{LS} values presented here differ from those proposed in Stefanidou & Kappos (2017) regarding the sample size used for the statistical analysis; the data included in the database is more extensive, as the sample size is larger, and hence the resulting values are more reliable.

Table 2. Uncertainties in limit state definition for bearings and abutments

	Bearings (Elastomeric) - $\gamma(\%)$				Abutments - $*(h_w)$			
	LS1	LS2	LS3	LS4	LS1	LS2	LS3	LS4
Mean	82.57	146.33	205.36	337.5	0.0046	0.0093	0.0367	0.081
Stand. Dev.	54.94	32.87	45.56	110.87	0.0026	0.0036	0.0111	0.0338
COV	0.67	0.22	0.22	0.33	0.57	0.39	0.3	0.42
β_{LS}	0.61	0.22	0.22	0.32	0.53	0.37	0.29	0.4
Average β_{LS} (LS1-LS4)	0.34				0.4			

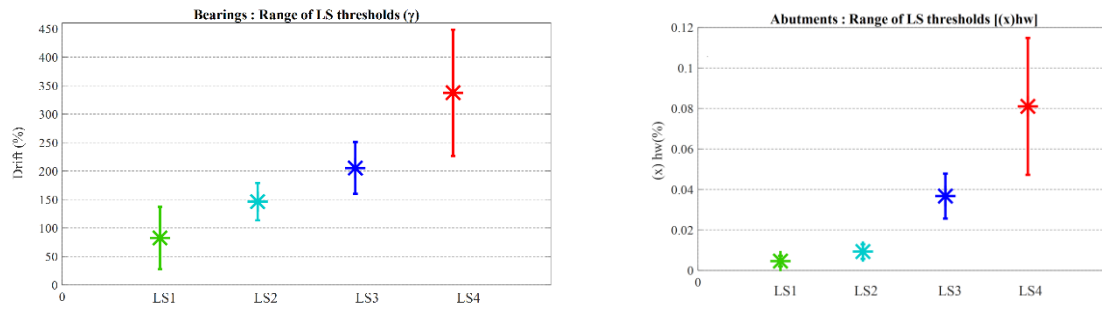


Figure 8. Range of LS thresholds for bearings and abutments

4.4. Online software for bridge-specific fragility analysis

4.4.1. Methodology for analysis using the simplified 3D bridge model

For the analysis of portfolios, bridge-specific fragility curves are calculated accounting for the fragility of all critical components using a 3D simplified elastic model (including the deck, piers, bearings, and abutments); response spectrum analysis is performed for the selected spectra, and the results are scaled to different levels of earthquake intensity.

The 3D elastic model set up in the platform is described in Fig. 9. Both deck and piers are modelled as elastic beam-column elements with user-defined geometry and section properties. Reduced stiffness is considered for bridge piers, estimated on the basis of section analysis which provides the secant flexural rigidity at yield $EI_{eff}=M_y/\phi_y$. Yield moment and curvature (M_y , ϕ_y) may also be calculated utilising the closed-form relationships proposed in §4.1.1 that account for the effect of varying geometric, material, and reinforcement properties. Bearings are modelled as springs with stiffness equal to that of all bearings considered at every support, while different boundary conditions are considered at the abutment for the case of open/closed gap (Fig. 10-right). The elastic model is clearly less accurate than the corresponding inelastic model; however, its reliability for fragility analysis of portfolios is deemed adequate since the bridge deformation shape is accurate and the effect of multiple modes on the results is accounted for (the number of modes considered is a user-defined parameter). The often adopted assumption of a single-degree-of-freedom model for bridges may be adequate for the longitudinal direction (approximately equal displacements at the pier tops for the case of stiff decks), but this is not

the case for the transverse direction, where the deformation pattern is strongly related to boundary conditions and the translational and rotational deck stiffness (Kappos et al. 2013).

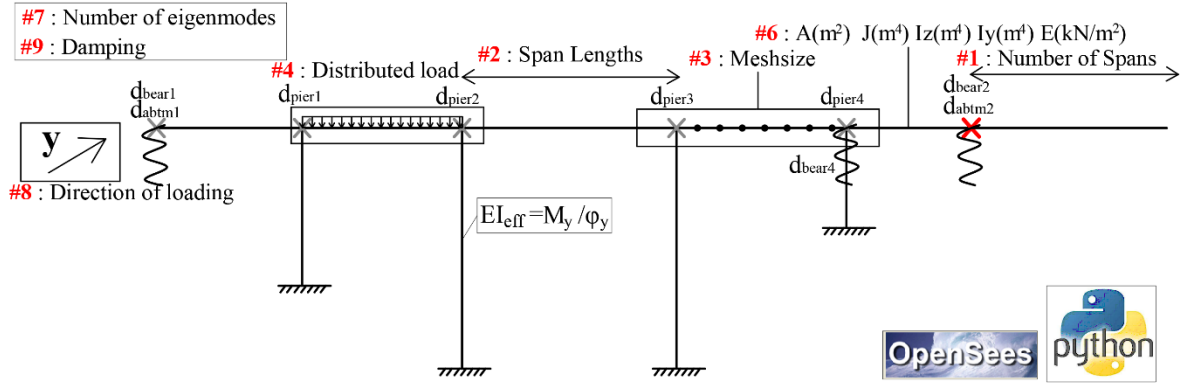


Figure 9. 3D simplified model for bridge-specific fragility analysis

For the estimation of bridge-specific fragility curves in the frame of the component-based methodology, seismic capacity (i.e. LS thresholds for minor to collapse limit state), demand, and uncertainties should be quantified for every critical component. The limit state thresholds for either as-built or retrofitted bridge piers are calculated from the closed-form relationships described in §4.1.1, accounting for all component-specific properties. The ratio of the height where pier moment equals zero (equivalent cantilever height) to the total pier height should be defined ($x=L_o/L$) to apply Eq. 1 and estimate limit state thresholds for restrained piers. In order to estimate the equivalent cantilever height, an initial analysis considering a loading pattern proportional to the predominant mode shape in each direction of the bridge (longitudinal, transverse) is applied. For the estimation of demand at component control points, response spectrum analysis is performed, and the results are scaled to varying levels of earthquake intensity (typically, PGA from 0.1 to 1g); the displacements at the control point of every critical component are recorded. Based on these response spectrum analysis results, the evolution of damage curve (or primary vulnerability curve) is plotted, and the $A_{g,m}$ and $A_{g,LS}$ values are estimated according to Fig. 10 (left). The total uncertainties for the bridge system are calculated according to §4.3. So long as capacity, demand, and uncertainties are estimated, fragility curves are plotted for all limit states (Eq. 3).

$$P_f = \Phi \left(\frac{1}{\sqrt{\beta_{tot}^2}} \cdot \ln \left(\frac{A_{g,m}}{A_{g,LS(i)}} \right) \right) \quad (3)$$

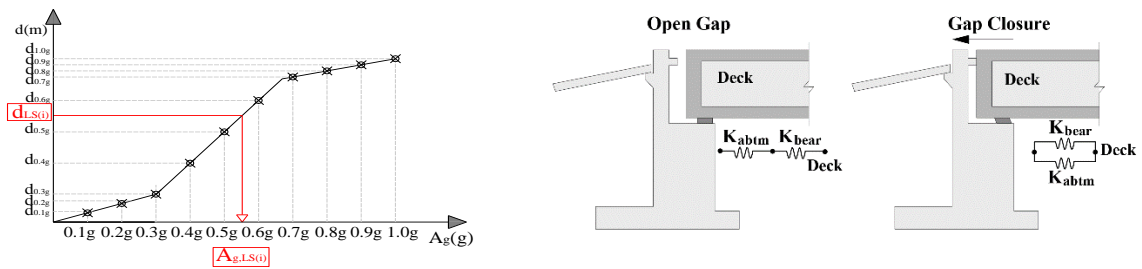


Figure 10. Evolution of damage (displacement demand versus earthquake parameter) (Left). Different boundary conditions before and after gap closure (Right)

4.4.2. Development of the online software (wizard) for bridge-specific fragility analysis

An online software (wizard) has been developed and included in the platform www.thebridgedatabase.com for the derivation of bridge-specific fragility curves, according to the methodology described in §4.4.1. The bridge geometry and the properties of piers, bearings, and abutments are defined on online forms and used as input to the parametrically defined bridge model in OpenSees.py. An ad-hoc software (in Python) has been developed, incorporating the features of the methodology described in the previous sections (model set up, limit state threshold estimation, response spectrum analysis, development of the evolution of damage curve, fragility curve estimation, etc.). The software is applicable to practically every straight bridge (up to 50 spans), with unequal spans, various deck geometries and pier-to-deck connection types. Both single and multi-column piers can be considered, with varying height and pier type (cylindrical, hollow cylindrical, rectangular, hollow rectangular, wall type). It is noted that only seat-type abutments are considered at this stage of development; these are the ones found in most bridges in Europe and other areas. The online software enables the user to calculate in real-time bridge-specific fragility curves for the longitudinal and transverse bridge direction (separately).

Generic 3d Elastic Model

1. Bridge Geometry (General Properties)
2. Pier Properties
3. Bearing Properties
4. Abutment Properties

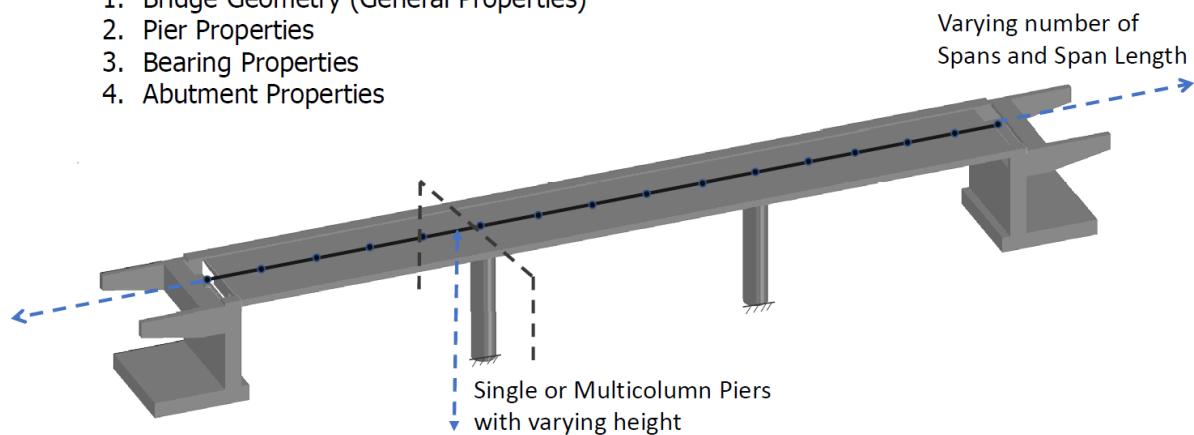


Figure 11. 3D generic bridge model and input parameters

The wizard consists of four online forms (Fig. 12) that should be filled in by the user. In the first form, general properties are defined, i.e., the number of spans, span lengths, pier heights, and deck geometry (at span and support location), along with properties related to seismic input (response spectrum), damping, and the number of modes considered. Regarding deck geometry, the properties defined for the support location are used as input for 15% of the span length (measured from piers or abutments) and the span properties in-between. It should be noted that the number of modes considered (related to the activated mass) is a critical parameter and should be defined by the user. The type of pier-to-deck connection is also defined, i.e., monolithic, through bearings, or a combination thereof, along with the total uncertainty value for each fragility curve. In the second form, the (single- or multi-column) pier type and properties are defined. For the estimation of the reduced pier stiffness, the effective flexural rigidity may be calculated based on the closed-form relationships proposed for M_y and ϕ_y , or user-defined values may be provided. Both as-built and retrofitted with RC or FRP jacket piers can be considered; both are defined using the same form. The following two forms refer to bearing and abutment properties, namely stiffness values (in either direction), bearing type and thickness, abutment stiffness (as proposed in Caltrans Guidelines or user-defined), backwall height, embankment soil type, and gap size. It is recalled that analyses considering two different boundary conditions are performed (Fig. 10, right), and the relevant results, before and after gap closure, are considered for the fragility curve estimation.

Based on the parameters defined in the online forms, the 3D model is set up, and response spectrum analysis for various PGA levels is performed for the derivation of bridge-specific fragility curves in the longitudinal and transverse direction (spectrum applied separately in each direction). Series connection between components is assumed for the derivation of bridge fragility curves, according to Eq. 4 (upper and lower bound, Zhang &Huo, (2009)):

$$\max_{i=1}^n [P(F_i)] \leq P(F_{system}) \leq 1 - \prod_{i=1}^n [1 - P(F_i)] \quad (4)$$

The lower bound corresponds to completely correlated components, while the upper bound assumes no correlation between components. Bridge fragility lies within these two bounds, and the exact value is dependent on the correlation of the component response. Both upper and lower bound bridge-specific fragility curves for all limit states are calculated by the online software and are displayed on the platform (Fig. 12).

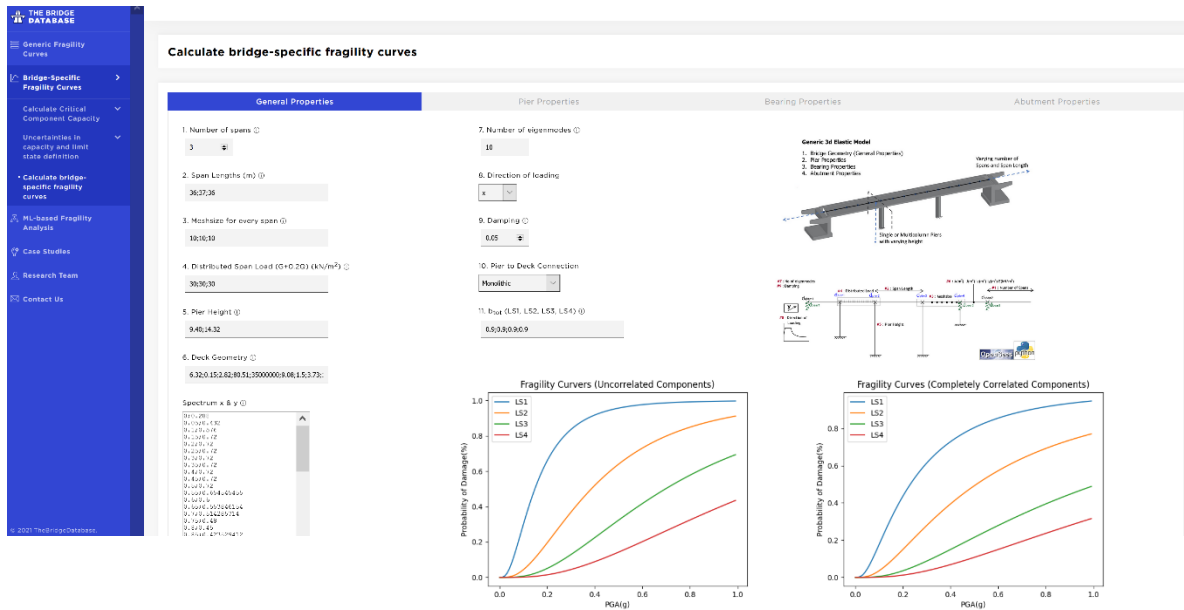


Figure 12. The online software for bridge-specific fragility analysis (online forms and fragility curves)

5. PILOT STUDY USING THE PLATFORM

The online platform is used to derive bridge-specific fragility curves for two bridges according to the methodology described in §4.4.1. The bridges selected have the same type of piers (cylindrical) and deck (RC slab), but different connection between the pier and the deck, i.e., either monolithic or through bearings (bridge classes 111 and 112 according to Stefanidou & Kappos, (2019)). It is noted that the time required for the real-time fragility curve calculation is less than 20sec for each bridge.

5.1. RC Bridge with cylindrical piers monolithically connected to deck slab (class 111)

The first case study is an overpass with concrete voided slab deck, single-column cylindrical piers, and monolithic pier-to-deck connection. The properties of the bridge critical components are presented in Fig. 14 and the pertinent completed online forms in Fig. 13. Geometric and material properties are provided, along with longitudinal and transverse reinforcement ratios and properties of the elastomeric bearings used at the abutments. The input values for effective bearing stiffness at abutment location, are estimated based on Naeim & Kelly (1999) and the longitudinal and transverse stiffness of the abutment-backfill system according to Caltrans (2010). The total uncertainties are estimated and presented in detail in Stefanidou & Kappos (2019) and are used as input in the relevant form.

Online estimation of the seismic fragility is performed, and the resulting fragility curve sets are presented in Fig. 14 for the four limit states considered. Both upper and lower bound fragilities are presented, according to Eq. 4, assuming series connection between components and uncorrelated or fully correlated components, respectively. It is recalled that the fragility of all critical components is first estimated and then used for the calculation of bridge-specific system fragility, considering the limit state thresholds adopted by the methodology described in §4.4.1, incorporated in the software.

General Properties

1. Number of spans

2. Span Lengths (m)

3. Meshsize for every span

4. Distributed Span Load (G+0.2Q) (kN/m²)

5. Pier Height

6. Deck Geometry

Spectrum x & y

0.288
0.358
0.432
0.516
0.600
0.696
0.804
0.936
1.104
1.320
1.584
1.900
2.280
2.736
3.288
3.960
4.776
5.760
7.056
8.712
10.752
13.200

Pier Properties

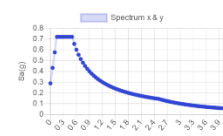
7. Number of eigenmodes

8. Direction of loading

9. Damping

10. Pier to Deck Connection

11. b_{tot} (LS1, LS2, LS3, LS4)

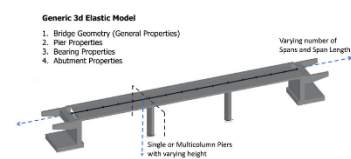
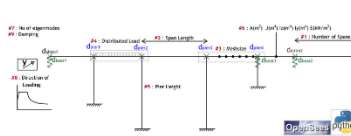


Bearing Properties

Abutmen

Generic 3d Elastic Model

- Bridge Geometry (General Properties)
- Pier Properties
- Bearing Properties
- Abutment Properties

General Properties

Pier type

Multi-column Piers: Number of piers

Multi-column Piers: Pier distance

Pier Number: #1

Pier to Deck Connection

Geometry

1.1 Pier Section Area (m²)

1.2 Moment of Inertia (m⁴) (Strong direction)

1.3 Moment of Inertia (m⁴) (Weak direction)

M_y-φ_y relationships (to account for reduced stiffness)

1.4 Torsional moment of Inertia (m⁴) [0.192]

1.5 Modulus of Elasticity (kN/m²)

1.6 M_y-φ_y

Closed form relationships M_y-φ_y values (as built parameters)

Bearings (Left Abutment)

1.1 K_y (kN/m)

1.2 K_{0x} (kN/m)

1.3 K_{0y} (kN/m)

1.4 K_{0z} (kNm/rad)

1.5 K_{0x} (kNm/rad)

1.6 K_{0y} (kNm/rad)

1.7 Bearing Type

1.8 Bearing Thickness (m)

Abutment #1 (Left)

1. K_{abtm,x} (kN/m)

2. K_{abtm,y} (kN/m)

3. Backwall height (m)

4. Gap_x (m)

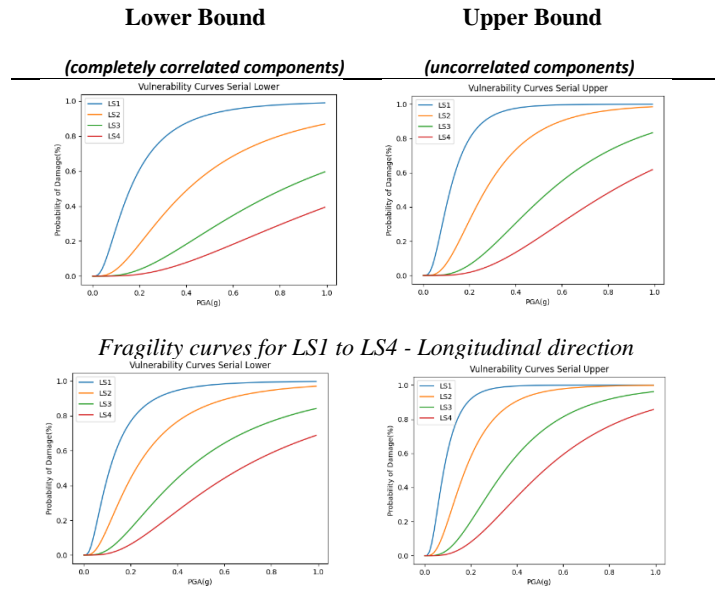
5. Gap_y (m)

6. Embankment Soil Type

Figure 13. Completed online forms for the case study bridge (class 111)

$$\max_{F_i} [P(F_i)] \leq P(F_{\text{system}}) \leq 1 - \prod_{i=1}^n [1 - P(F_i)]$$

Overpass Bridge G5 (OP 08.13.14)	
Category 111 (Classification Stefanidou&Kappos, 2019)	
Bridge Sketch	
Deck [X2:1]	
Type	Slab
Deck Concrete	C30/37
Piers [X1:1]	
Type	Single Column - Cylindrical
Diameter (m)	D=1.60
Area (m ²)	2.01
Pier Concrete	C30/37
Pier Steel	S500s
Long. Reinf. Ratio	$\rho_l=0.0117$
Transv. Reinf. Ratio	$\rho_w=0.006$
Pier-to-deck connection : Monolithic [X3:1]	
Abutment Bearings	
Bearing Type	Elastomeric
Dimension (mm)	400×400×77 (7 layers/11mm each)
*t : total elastomer height	
Foundation Soil Type	
B (EC8)	



Fragility curves for LS1 to LS4 - Transverse direction

Figure 14. Bridge and component properties and fragility curves (lower & upper bound) for the case study bridge (class 111) in the longitudinal direction

5.2. RC Bridge with cylindrical piers connected through bearings to deck slab (class 112)

The second case study is an overpass with deck slab, single-column cylindrical piers, and pier-to-deck connection through bearings. The properties of the bridge critical components are presented in Fig. 16 and the relevant completed online forms in Fig. 15. Geometric and material properties are provided along with longitudinal and transverse ratios and elastomeric bearing properties at piers and abutments. The input values for effective bearing stiffness and the longitudinal and transverse stiffness of the abutment-embankment system are estimated as described in §5.1. The total uncertainties are estimated and presented in detail in Stefanidou & Kappos (2019) and are used as input in the relevant form.

General Properties

1. Number of spans

2. Span Lengths (m)

3. Meshsize for every span

4. Distributed Span Load (G+0.2Q) (kN/m²)

5. Pier Height

6. Deck Geometry

Spectrum x & y

Pier Properties

7. Number of eigenmodes

8. Direction of loading

9. Damping

10. Pier to Deck Connection

11. Drest (LS1, LS2, LS3, LS4)

Bearing Properties

Generic 3D Elastic Model

- Bridge Geometry (General Properties)
- Pier Properties
- Bearing Properties
- Abutment Properties

Pier Properties (Pier #1)

Pier to Deck Connection

Geometry

1.1 Pier Section Area (m²) 1.4 Torsional moment of Inertia (m⁴) [-0.10]

1.2 Moment of Inertia (m⁴) [Strong Direction] 1.5 Modulus of Elasticity (kN/m²)

1.3 Moment of Inertia (m⁴) [Weak Direction]

M_y-φ_y relationships (to account for reduced stiffness)

1.6 M_y - φ_y

Closed form relationships M_y - φ_y values (as built parameters)

1.7 Pier Section 1.11 f_c (MPa)

1.8 D (m) 1.12 f_y (MPa)

1.9 d (m) 1.13 ρ_s

1.10 f_{cm} 1.14 d_w

Bearings (Left Abutment)

1.1 K_y (kN/m) 1.5 K_{B,x} (kNm/rad)

1.2 K_{H,x} (kN/m) 1.6 K_{B,y} (kNm/rad)

1.3 K_{H,y} (kN/m) 1.7 Bearing Type

1.4 K_{B,z} (kNm/rad) 1.8 Bearing Thickness (m)

Abutment #1 (Left)

1. K_{abotm,x} (kN/m) 4. Gap_x (m)

2. K_{abotm,y} (kN/m) 5. Gap_y (m)

3. Backwall height (m) 6. Embankment Soil Type

Figure 15. Completed online forms for the case study bridge (class 112)

The online estimation of the seismic fragility is performed, and the resulting fragility curve sets are presented in Fig. 16.; similar comments apply as in the previous case study.

$$\max_{i=1}^n [P(F_i)] \leq P(F_{\text{system}}) \leq 1 - \prod_{i=1}^n [1 - P(F_i)]$$

Overpass Bridge (OP 04.09.09A)	
Category 112 (Classification Stefanidou&Kappos, 2019)	
Bridge Sketch	
Deck [X2:1]	
Type	Slab
Deck Concrete	C30/37
Piers [X1:1]	
Type	Single Column - Cylindrical
Diameter (m)	D=2.00
Area (m ²)	3.14
Pier Concrete	C20/25
Pier Steel	S500s
Long. Reinf. Ratio	$\rho_l=0.0181$
Transv. Reinf. Ratio	$\rho_w=0.005$
Pier-to-deck connection : Bearing [X3:2]	
Bearing Type	Elastomeric
Dimension (mm)	900×900×126 (7×18)
**†: total elastomer height	
Abutment Bearings	
Bearing Type	Elastomeric
Dimension (mm)	4 bearings 30×40×80 (10x8mm)
**†: total elastomer height	
Foundation Soil Type	
B (EC8)	

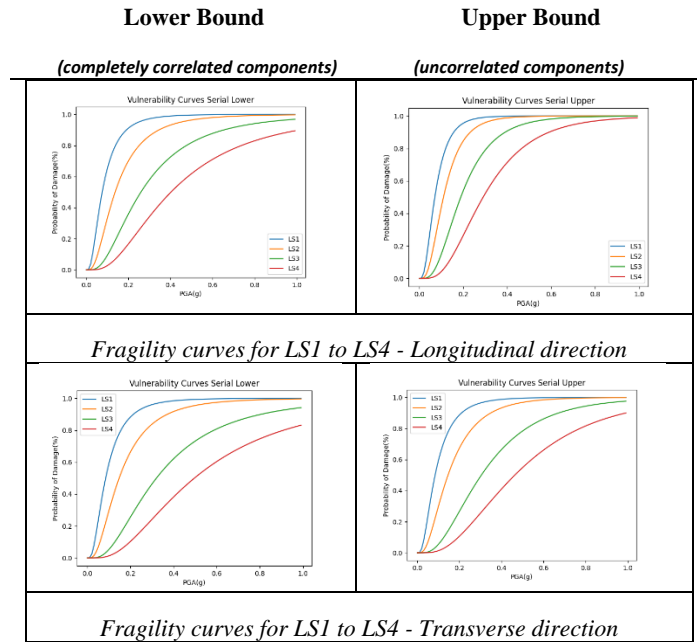


Figure 16. Bridge and component properties and fragility curves (lower & upper bound) for the case study bridge (class 112) in the longitudinal direction

6. CONCLUSIONS

An online platform (www.thebridgedatabase.com) developed for fragility assessment of as-built and retrofitted bridges were presented; it constitutes the first open-access platform for real-time analytical estimation of bridge-specific fragility curves. The platform is ‘two-track’, including ad-hoc software for online bridge-specific fragility analysis, as well as the option to select an appropriate set of generic fragility curves from a database, including a variety of bridge classes. It is fully interactive, allowing input from users/contributors with a view to enriching the database and receiving feedback. Moreover, a detailed approach for the estimation of component-specific limit state thresholds is provided, including extensive lists with thresholds for all critical components (from experimental studies) as well as closed-form relationships and a parametrically defined pier model for capacity assessment and estimation of limit state thresholds for as-built and retrofitted piers. The software for bridge-specific fragility assessment performs analysis of a fully parameterised model bridge model, set up according to user-defined (through user-friendly online forms) geometry, component parameters, and seismic excitation input. A software, including the probabilistic framework for fragility analysis and all relevant features, was also developed, enabling the online, real-time estimation of bridge-specific fragility curves for each direction of the bridge. An application of the platform to two case-study bridges was presented and highlighted its applicability to bridges with varying structural systems and properties. The software is open access, and it can be claimed that it makes feasible (for the first time) the derivation of bridge-

specific fragility curves for entire bridge portfolios; hence, it can be used (free of charge) by professionals and researchers for decision-making or in the frame of bridge/roadway network resilience analysis.

ACKNOWLEDGEMENTS

“This research was co-financed by Greece and the European Union (European Social Fund- ESF) through the Operational Programme «Human Resources Development, Education and Lifelong Learning 2014- 2020» in the context of the project “*Online database for the development of fragility curves for as-built and retrofitted RC bridges using machine learning techniques*” (MIS 5047878).



REFERENCES

- Berry, M., & Eberhard, M. (2003). *Performance Models for Flexural Damage in Reinforced Concrete Columns* (Issue August).
- Bisadi, V., Head, M., & Gardoni, P. (2011). Seismic Fragility Estimates and Optimization of Retrofitting Strategies for Reinforced Concrete Bridges: Case Study of the Fabela Bridge in Toluca, Mexico. *Structures Congress 2011, ASCE*, 13–22. [https://doi.org/10.1061/41171\(401\)2](https://doi.org/10.1061/41171(401)2)
- Caltrans Structures Seismic Design Criteria. (2010). Sacramento, California.
- Crowley, H., Colombi, M., Silva, V., Monteiro, R., Ozcebe, S., Fardis, M., Tsionis, G., & Askouni, P. (2011). *SYNER-G : Systemic Seismic Vulnerability and Risk Analysis for Buildings, Lifeline Networks and Infrastructures Safety Gain*.
- D’Ayala, D., Gehl, P., & et al. (2015). *INFRARISK: Novel Indicators for identifying critical Infrastructure at Risk from Natural Hazards - Deliverable D3.2 - Fragility Functions Matrix*.
- DesRoches, R., Padgett, J., Ramanathan, K., & Dukes, J. (2012). *Feasibility Studies for Improving Caltrans Bridge Fragility Relationships* (Vol. 0003, Issue 2).
- Dwairi, H., & Kowalsky, M. J. (2004). Inelastic displacement patterns in support of displacement-based design for multispan bridges. *13th World Conference on Earthquake Engineering*, 231.
- EN1992-1-1, Eurocode 2: design of concrete structures – Part 1-1: General rules and rules for buildings, European Committee for Standardization, 2004.* (n.d.).
- FEMA-NIBS (2003) Multi-hazard Loss Estimation Methodology - Earthquake Model: HAZUS®MH Technical Manual, Washington DC.*
- Kappos, A.J., Gkatzogias, K.I., and Gidaris, I. “Extension of direct displacement-based design

- methodology for bridges to account for higher mode effects”, Earthquake Engineering & Structural Dynamics, V. 42, no.4, Apr. 2013, 581–602. DOI: 10.1002/eqe.2229 (13-7-2012)
- Mander, J. B., Priestley, M. J. N., & Park, R. (1988). Theoretical Stress-Strain Model for Confined Concrete. *Journal Of Structural Engineering*, 114(8), 1804–1826.
- Mergos, P. E., & Kappos, A. J. (2009). Seismic damage analysis including inelastic shear–flexure interaction. *Bulletin of Earthquake Engineering*, 8(1), 27–46. <https://doi.org/10.1007/s10518-009-9161-2>
- Mohammadi, K., & Lahijanian, H. (2010). Fragility Curves of Bridges Before and after Retrofitting by FRP. *5th Civil Engineering Conference in the Asian Region and Australasian Structural Engineering Conference*.
- Moschos, I. F., Kappos, A. J., Panetsos, P., Papadopoulos, V., Makarios, T., & Thanopoulos, P. (2008). Seismic fragility curves for greek bridges: methodology and case studies. *Bulletin of Earthquake Engineering*, 7(2), 439–468. <https://doi.org/10.1007/s10518-008-9077-2>
- Muntasir Billah, a. H. M., & Shahria Alam, M. (2014). Seismic fragility assessment of highway bridges: a state-of-the-art review. *Structure and Infrastructure Engineering*, June, 1–29. <https://doi.org/10.1080/15732479.2014.912243>
- Naeim, F., & Kelly, J. M. (1999). *Design of Seismic Isolated Structures*. John Wiley & Sons, INC., U.S.A.
- Silva, V., Crowley, H., & Colombi, M. (2014). Fragility function manager tool. In *SYNER-G: Typology Definition and Fragility Functions for Physical Elements at Seismic Risk*, Springer. <https://doi.org/10.1007/978-94-007-7872-6>
- Spolstra, B. M. R., & Monti, G. (1999). FRP-Confined Concrete Model. *Journal of Composites for Construction*, 3(3), 143–150.
- Stefanidou, S.P., & Kappos, A. J. (2019). Bridge Specific Fragility Analysis: When is it really necessary? *Bulletin of Earthquake Engineering*, 17(4), 2245–2280.
- Stefanidou, Sotiria P., & Kappos, A. J. (2021). Fragility-informed selection of bridge retrofit scheme based on performance criteria *Engineering Structures*. 234, May 2021; <https://doi.org/10.1016/j.engstruct.2021.111976>
- Stefanidou, Sotiria P., & Kappos, A. J. (2017). Methodology for the development of bridge-specific fragility curves. *Earthquake Engineering & Structural Dynamics*, 46, 73–93. <https://doi.org/10.1002/eqe>
- Tsionis, G., & Fardis, M. N. (2012). Seismic Fragility of Concrete Bridges with Deck Monolithically Connected to the Piers or Supported on Elastomeric Bearings. *15th World Conference of Earthquake Engineering*.
- Van Rossum, G., & Drake, F. L. (2009). Python 3 Reference Manual. *Scotts Valley, CA: CreateSpace*.
- Yepes-Estrada, C., Silva, V., Rossetto, T., D’Ayala, D., Ioannou, I., Meslem, A., & Crowley, H. (2016). The global earthquake model physical vulnerability database. *Earthquake Spectra*, 32(4), 2567–2585. <https://doi.org/10.1193/011816EQS015DP>
- Zhang, J., & Huo, Y. (2009). Evaluating effectiveness and optimum design of isolation devices for highway bridges using the fragility function method. *Engineering Structures*, 31(8), 1648–1660. <https://doi.org/10.1016/j.engstruct.2009.02.017>
- Zhu, M., McKenna, F., & Scott, M. H. (2018). OpenSeesPy: Python library for the OpenSees finite element framework. *SoftwareX*, 7, 6–11. <https://doi.org/10.1016/j.softx.2017.10.009>